Observation of equatorial Kelvin solitary waves in a slowly varying thermocline

Q. Zheng, R. D. Susanto, X.-H. Yan, W. T. Liu, C.-R. Ho

Nonlinear Processes in Geophysics (1998) 5: 153–165

Nonlinear Processes in Geophysics

Observation of equatorial Kelvin solitary waves in a slowly varying thermocline

Q. Zheng[1], R. D. Susanto[1,*], X.-H. Yan[1], W. T. Liu[2] and C.-R. Ho[3]

[1]Center for Remote Sensing, Graduate College of Marine Studies, University of Delaware, Newark, DE 19716, USA
*Currently at Lamont-Doherty Earth Observatory of Columbia University, Palisades, NY 10964, USA
[2]Jet Propulsion Laboratory, California Institute of Technology, Pasadena, CA 91109, USA
[3]Department of Oceanography, National Taiwan Ocean University, Keelung 202, Taiwan

Received: 15 January 1998 – Accepted: 15 October 1998

Abstract. TOPEX/POSEIDON (T/P) sea level deviation (SLD) time series from October 3, 1992 to May 15, 1997 combined with upper ocean thermal structures are used to observe the characteristics and analyze the dynamics of equatorial waves in the Pacific Ocean. The evolution of the Kelvin wave propagating along an eastward shoaling thermocline in the equatorial Pacific is investigated. The behavior of this wave as it propagates eastward can be approximately described with the solutions of the perturbed Korteweg-de Vries (PKdV) equation and modified Green's Law. Assuming that the nonlinear term and dispersive term of this equation are balanced, the amplitude increases as the thermocline decreases to the power $-3/8$. Approaching the eastern Pacific, the nonlinearity increases and the relation changes to the power $-9/8$. The dispersion relation, and mass and energy conservations are investigated. The results indicate that under a varying thermocline, the nonlinear Kelvin solitary waves indeed exist in the real ocean.

1 Introduction

Linear equatorial waves theories (i.e. Moore and Philander, 1977; Pedlosky, 1987; Philander, 1990) have assumed that these waves propagate in an ocean with a horizontally uniform stratification. Hydrographic observations indicate that the density field in the tropical oceans varies not only vertically, but also horizontally. A prominent feature in the equatorial Pacific Ocean is an eastward shoaling thermocline depth (Gill, 1982; Cushman-Roisin, 1994). As a first approximation, this tilted thermocline can be thought of as a result of a simple balance between the zonal wind forcing and the pressure gradient (Long and Chang, 1990).

Hughes (1981) has studied the influence of a zonal slope in the thermocline on both wave- and wind-induced equatorial upwelling using a linear $1\frac{1}{2}$-layer reduced gravity model. He derived a simple relation between the amplitude of a Kelvin wave and the thermocline depth based on the energy conservation law. The zonal velocity and the wave height vary as the thermocline depth to the power $-7/8$ and $-3/8$, respectively. Using a linear $2\frac{1}{2}$-layer reduced gravity model, Gill and King (1985) investigated the energy transfer between Kelvin wave vertical modes as the wave propagates into a shoaling thermocline. Using a numerical approach, they concluded that, for the high frequency waves, there is very little energy transfer between modes. However, for the low frequency waves that are associated with an El Niño event, there is significant energy transfer between modes. Busalacchi and Cane (1988) have investigated the same problem using a linear continuously-stratified model. They concluded that the zonally varying thermocline does not produce significant changes in the energy flux, but can cause significant change in the amplitudes of equatorial waves.

It is worth noting that the studies described above have assumed that the equatorial waves are linear and periodic in time. In the real ocean, however, the observed Kelvin waves are closely correlated with impulsive changes in the wind forcing, and thus propagate in the form of wave fronts (Ripa and Hayes, 1981; Knox and Halpern, 1982; Eriksen et al., 1983; Lukas et al., 1984). The fundamental difference between a periodic wave and a wave front is that a wave front carries both energy and mass, whereas a periodic wave does not carry mass. A number of theoretical studies, reviewed by Boyd (1990), have predicted that equatorial waves may exist in the frame of the nonlinear shallow water equations. Boyd (1980) indicated that weakly nonlinear equatorial Rossby waves satisfy either the Korteweg-de Vries (KdV) equation or the modified Korteweg-de Vries (MKdV) equation, which are derived from the nonlinear shallow water equations and have soliton solutions. Boyd (1983) showed that equatorial Rossby en-

Correspondence to: Q. Zheng

velope solitons exist theoretically; the meridional structure is the same as that of linear waves and the zonal-temporal structure behaves as a single soliton that satisfies the nonlinear Schödinger equation. Marshall and Boyd (1987) extended Boyd's studies to include the effects of continuous vertical stratification. Boyd (1984) and Greatbatch (1985) indicated that the equatorial Kelvin solitons can be derived from the shallow water equations if a shear mean flow is included in the zonal component of the velocity.

Kindle (1983) demonstrated that equatorial Rossby solitary waves can be excited by a relaxation of the equatorial winds in a nonlinear, one-layer, reduced-gravity model of the tropical Pacific Ocean. Greatbatch (1985) simulated the generation of equatorial Rossby waves by a sudden onset of spatially-uniform winds in a model equatorial ocean basin. These numerical simulations show an agreement with theoretical predictions by Boyd (1980, 1984). Long and Chang (1990) considered the effect of a slow zonal variation in thermocline depth on the propagation of a finite-amplitude Kelvin wave pulse in a single layer model, and showed that the amplitude of the pulse satisfies the perturbed KdV (PKdV) equation, which has a solitary solution (Newell, 1985). They also gave the visualized forms of the solution using numerical methods. Glazman et al. (1996) observed a nonlinear feature of baroclinic Rossby waves from the T/P sea level data.

Solitary internal Kelvin waves have also been simulated in the laboratory. Maxworthy (1983) simulated solitary internal Kelvin waves using a rotating channel with a stratified shallow fluid and measured the structure and properties of the waves. Renouard et al. (1987) and Melville et al. (1990) also simulated the generation and evolution of nonlinear internal Kelvin waves with a two-layer flow in the laboratory. These laboratory simulations showed that solitary Kelvin waves are a stable oscillation mode.

The above-mentioned results, however, are restricted to theoretical prediction and numerical or laboratory simulations. The modeled or simulated equatorial Kelvin solitary waves have never been observed in the real ocean. Probably the main reason for this is the lack of measurements of the real ocean with the accuracy, and the temporal and spatial resolutions, necessary for these kinds of observations.

Data from the T/P altimeter, the most accurate altimeter ever flown with unprecedented orbit and altimeter accuracies, are available. We will verify, using the approach of Long and Chang (1990), and the T/P sea level deviation data, that there are indeed nonlinear equatorial Kelvin solitary waves in the Pacific Ocean.

2 Equatorial Solitary Kelvin Waves in a Slowly Varying Thermocline

The eastward shoaling thermocline depth along the equatorial Pacific Ocean is a prominent feature. However, traditional equatorial wave theories were derived based on an assumption that the ocean has a horizontally uniform thermocline. Thus the effects of the shoaling thermocline on the waves in the real ocean were disregarded (for example Moore and Philander, 1977; Pedlosky, 1987; Philander, 1990).

Using first order perturbation equations for a two-layer model ocean, Hughes (1981) found that, based on the energy conservation law, the amplitude of linear Kelvin waves increases as the thermocline depth decreases to the power $-3/8$. The wave amplitude has to increase as the thermocline depth decreases in order to conserve energy. Hence, the nonlinearities will be enhanced as the wave propagates through a shoaling thermocline depth. However, Hughes (1981) ignored the nonlinearity effect. Long and Chang (1990) examined the effects of the thermocline on the propagation of the equatorial Kelvin waves in the Pacific Ocean while including the nonlinearity effect. They found that the Kelvin waves evolve into solitary waves of Korteweg-de Vries (KdV) type, as they propagate in the ocean with an eastward shoaling thermocline, if the dispersion caused by the meridional variation of the layer depth is considered.

In this research, following Long and Chang (1990), field data of both zonal and meridional thermocline depths combined with T/P SLD data are used to investigate thermocline effects on the Kelvin wave propagation in the equatorial Pacific Ocean.

2.1 Governing Equations and Solutions

The model geometry adopted in this research is a $1\frac{1}{2}$-layer model which consists of one active layer of density ρ_1 above a resting infinitely deep layer of density ρ_2, with $\rho_1 < \rho_2$. To simplify the analysis, the equations are nondimensionalized by choosing $C_o = \sqrt{g' H_o}$, the internal phase speed of the upper layer, as the unit velocity. H_o is the equilibrium of the upper active layer thickness. $L_e = \sqrt{C_o/\beta}$, the equatorial Rossby radius of deformation, as the unit of length. The study area is in the equatorial Pacific Ocean, therefore the Coriolis parameter $f(y)$ can be approximated by the equatorial β-plane, i.e. $f(y) = \beta y$.

The nondimensionalized nonlinear shallow water wave equations, under a Boussinesq, hydrostatic, reduced gravity ocean, on the equatorial β-plane that are wind forced, are given in the following form:

$$\begin{aligned} u_t + uu_x + vu_y - yv &= -h_x + \tau^x, \\ v_t + uv_x + vv_y + yu &= -h_y + \tau^y, \\ h_t + (uh)_x + (vh)_y &= 0, \end{aligned} \tag{1}$$

where u and v are zonal and meridional components of

velocity fields, respectively, h is the total upper layer thickness, τ^x and τ^y are the zonal and meridional component of wind forcings, respectively. The subscripts denote differentiation with respect to the subscripted variable.

Since the objective of this research is to investigate the effects of a shoaling thermocline on Kelvin wave propagation along the equatorial Pacific Ocean, the background current that might affect the waves propagation is neglected. Thus, the momentum equations are a balance between wind forcings and the pressure gradient.

Following a model by Long and Chang (1990) who introduced a small amplitude parameter ϵ for wave disturbances, and assuming that the amplitude of the zonal and meridional wind forcings are of $O(1)$ and $O(\epsilon^{1/2})$, respectively, then the basic state solution can be written as follows:

$$\begin{aligned} \bar{u} &= 0, \\ \bar{v} &= 0, \\ \bar{h} &= H(x) + \epsilon^{1/2}\Psi(y), \end{aligned} \tag{2}$$

with $H_x = \tau^x$ and $\epsilon^{1/2}\Psi_y = \tau^y$, where both $H(x)$ and $\Psi(y)$ are of $O(1)$. One can write u, v, and h as their mean values plus a small perturbation of $O(\epsilon)$. The perturbation equations for Eqs. (1) become

$$\begin{aligned} u_t &+ \epsilon(uu_x + vu_y) - yv = -h_x, \\ v_t &+ \epsilon(uv_x + vv_y) + yu = -h_y, \\ h_t &+ (C^2 + \epsilon^{1/2}\Psi)(u_x + v_y) + 2CC_x u + \epsilon^{1/2}\Psi_y v \\ &+ \epsilon[(hu)_x + (hv)_y] = 0, \end{aligned} \tag{3}$$

where $C(x) = [H(x)]^{1/2}$ is the local shallow water wave speed in the absence of meridional variation Ψ. The total shallow water wave speed C_s is give by $C_s = \sqrt{h} = (C^2 + \epsilon^{1/2}\Psi)^{1/2}$. One can see that an $O(\epsilon^{1/2})$ meridional variation in the layer depth contributes an $O(\epsilon^{1/2})$ correction to the local shallow water phase speed $C(x)$, if there is no meridional variation of thermocline depth Ψ.

A multiple scale analysis (Shen, 1993) is used to solve Eqs. (3) by introducing fast and slow scales for both time and spatial scales,

$$t \Rightarrow t + \epsilon^{1/2}\omega_1 t + \epsilon\omega_2 t + \ldots = t + \varpi_1 + \varpi_2 + \ldots, \tag{4}$$

$$x \Rightarrow x + \epsilon x + \ldots = x + \chi + \ldots, \tag{5}$$

where ω_n are the corrections of phase speed $C(x)$, and a proper characteristic coordinate for wave propagations. One may assume that a wave propagating to the right and left will have a form,

$$\begin{aligned} \eta &= f(\zeta, \chi, \varpi), \\ \eta &= f(\sigma, \chi, \varpi), \end{aligned} \tag{6}$$

respectively, where

$$\begin{aligned} \zeta &= \int k\,dx - \omega t, \\ \sigma &= \int k\,dx + \omega t, \end{aligned} \tag{7}$$

and where χ and ϖ represent slow variation in x and t. Noting that $k = \frac{\omega}{C(x)}$, where $C(x) = H(x)^{1/2}$, and one may alternatively define ζ and σ as,

$$\begin{aligned} \zeta &= t - \int^x \frac{dx}{C(\epsilon x)} = t - \frac{1}{\epsilon}\int^\chi \frac{d\chi}{H^{1/2}(\chi)}, \\ \sigma &= t + \int^x \frac{dx}{C(\epsilon x)} = t + \frac{1}{\epsilon}\int^\chi \frac{d\chi}{H^{1/2}(\chi)}, \end{aligned} \tag{8}$$

where $H(x) = H(\epsilon\chi)$ is the thermocline depth, which is a slowly-varying function of x.

After applying the derivatives of these fast and slow variables using the chain rule, Eqs. (3) become

$$\begin{aligned} \left(u + \frac{h}{C}\right)_\sigma &+ \left(u - \frac{h}{C}\right)_\zeta - yv + \epsilon^{1/2}\omega_1(u_\sigma + u_\zeta) \\ &+ \epsilon\omega_2(u_\sigma + u_\zeta) + \epsilon h_\chi + \epsilon\frac{1}{C}u(u_\sigma - u_\zeta) \\ &+ \epsilon v u_y + \epsilon^2 u u_\chi = 0. \end{aligned} \tag{9}$$

$$\begin{aligned} (v_\sigma + v_\zeta) &+ yu + h_y + \epsilon^{1/2}\omega_1(v_\sigma + v_\zeta) + \epsilon\omega_2(v_\sigma + v_\zeta) \\ &+ \epsilon\frac{1}{C}u(v_\sigma - v_\zeta) + \epsilon v v_y + \epsilon^2 u v_\chi = 0. \end{aligned} \tag{10}$$

$$\begin{aligned} \left(u + \frac{h}{C}\right)_\sigma &- \left(u - \frac{h}{C}\right)_\zeta + Cv_y + \epsilon^{1/2}\omega_1\frac{1}{C}(h_\sigma + h_\zeta) \\ &+ \epsilon^{1/2}\frac{\Psi}{C^2}(u_\sigma - u_\zeta) + \epsilon^{1/2}\frac{1}{C}(\Psi v)_y \\ &+ \epsilon\omega_2\frac{1}{C}(h_\sigma + h_\zeta) + \epsilon C u_\chi + 2\epsilon C_\chi u \\ &+ \epsilon\frac{1}{C^2}[(uh)_\sigma - (uh)_\zeta] + \epsilon\frac{1}{C}(vh)_y \\ &+ \epsilon^{3/2}\frac{1}{C}\Psi u_\chi + \epsilon^2\frac{1}{C}(uh)_\chi = 0. \end{aligned} \tag{11}$$

Equations (9) to (11) represent the perturbed equations of motion in the new coordinate system, where the approximate solutions can be determined using an asymptotic expansion.

Collecting all the terms of $O(1)$ in Eqs. (9) to (11), the lowest order solutions are:

$$\begin{aligned} \left(u_o + \frac{h_o}{C}\right)_\sigma + \left(u_o - \frac{h_o}{C}\right)_\zeta - yv_o &= 0, \\ \frac{\partial v_o}{\partial\sigma} + \frac{\partial v_o}{\partial\zeta} + yu_o + \frac{\partial h_o}{\partial y} &= 0, \\ \left(u_o + \frac{h_o}{C}\right)_\sigma - \left(u_o - \frac{h_o}{C}\right)_\zeta + C\frac{\partial v_o}{\partial y} &= 0. \end{aligned} \tag{12}$$

These are the equations governing linear equatorial waves. Since the objective of this research is to investigate the equatorial Kelvin waves propagating eastward along the characteristic ζ constant (which means $\frac{\partial}{\partial\sigma}=0$) and admits a solution with zero meridional flow ($v=0$), then Eqs. (12) have solutions in the following form :

$$\begin{aligned} u_o &= A(\zeta,\chi)e^{-\frac{1}{4}Y^2(\chi,y)}, \\ v_o &= 0, \\ h_o &= C(\chi)A(\zeta,\chi)e^{-\frac{1}{4}Y^2(\chi,y)}, \end{aligned} \tag{13}$$

where $Y=[2/C(\chi)]^{1/2}y$, and A is amplitude. One can see that these are exactly the same as the solutions of linear Kelvin wave theory. Thus, a linear Kelvin wave in the presence of a varying thermocline can be obtained at the lowest order solution.

After calculating the higher orders $O(\epsilon^{1/2})$ and $O(\epsilon)$, the perturbed KdV equation is obtained (Long and Chang, 1990),

$$C\frac{\partial A}{\partial\chi}+\frac{7}{4}\frac{\partial C}{\partial\chi}A-\left(\frac{3}{2}\right)^{1/2}\frac{1}{C}A\frac{\partial A}{\partial\zeta}-M\frac{\partial^3 A}{\partial\zeta^3}=0, \tag{14}$$

with

$$M = \frac{1}{4C^5}\sum_{n=1}^{\infty}(n-1)!{\varphi_n}^2, \quad \text{and} \tag{15}$$

$$\varphi_n = \frac{1}{n!\sqrt{2\pi}}\int_{-\infty}^{\infty}D_n(Y)\Phi(Y)D_o(Y)\,dY. \tag{16}$$

where $D_n(Y)$ are parabolic cylinder functions and $\Phi(Y)$ is the variation of meridional thermocline depth.

Equation (14) is the final form of the perturbed KdV (PKdV) equation in a varying thermocline depth which includes both zonal and meridional variations of thermocline depth. The first two terms represent the shoaling of the thermocline, the third term is the nonlinearity effect, and the last term represents the dispersion effect. One can see that the nonlinearity and dispersion terms both appear at $O(\epsilon)$. This is the reason why an $O(\epsilon^{1/2})$ of the meridional variation in the thermocline depth is chosen.

Equation (14) can be transformed to the form of the PKdV equation by introducing a transform

$$A(\chi,\zeta)=\left(\frac{2}{3}\right)^{1/2}H^{3/2}q(\theta,\tau), \tag{17}$$

where

$$\tau = \frac{1}{6}\int^{\chi}H^{1/2}\,d\chi, \tag{18}$$

$$\theta = -\zeta=-t+\frac{1}{\epsilon}\int^{\chi}\frac{d\chi}{H^{1/2}(\chi)}. \tag{19}$$

Then we have

$$q_\tau+6qq_\theta+\frac{6M}{H}q_{\theta\theta\theta}=-\frac{19}{8}\frac{H_\tau}{H}q. \tag{20}$$

The evolution amplitude q depends on zonal thermocline depth H. τ is a rescaled zonal distance coordinate and θ is a negative retarded time.

The standard form of the PKdV equation for nonlinear surface gravity waves in a shoaling beach is given by Newell (1985)

$$q_\tau+6qq_\theta+q_{\theta\theta\theta}=-\frac{9}{4}\frac{H_\tau}{H}q, \tag{21}$$

Comparing with Eq. (21), let the coefficient of the third term on the left hand side of Eq. (20) be 1, which yields a confined condition

$$M=\frac{H}{6}=\frac{C^2}{6}. \tag{22}$$

Finally, the PKdV equation for a nonlinear Kelvin solitary wave is

$$q_\tau+6qq_\theta+q_{\theta\theta\theta}=-\frac{19}{8}\frac{H_\tau}{H}q, \tag{23}$$

One can see that there is a slightly different coefficient on the right hand side of Eqs. (23) and (21). The coefficient in Eq. (23) is 5.5% larger than that in Eq. (21). The standard PKdV equation in Eq. (21) has an analytical solution (Newell, 1985), and therefore, in the following analysis, the wave solution of Eq. (21) is a good approximation of the solution to Eq. (23). In addition, it is suitable for comparison with satellite observations. The analytical solution of Eq. (21), with $\frac{H_\tau}{H}$ is of order μ where $0<\epsilon\ll\mu\ll 1$, is

$$q(\theta,\tau)=q^{(0)}(\theta,\tau)+\mu q^{(1)}(\theta,\tau)+\ldots, \tag{24}$$

and the 0−order solution is

$$q^{(0)}(\theta,\tau)=2\eta^2\mathrm{sech}^2\eta(\theta-4\eta^2\tau-\theta_o), \tag{25}$$

while the 1−order solution is

$$\begin{aligned} q^{(1)} = {} & \frac{\Gamma}{6\eta}\Big\{-1+\tanh(\eta\xi)+\mathrm{sech}^2\eta\xi[3-3\eta\xi\tanh(\eta\xi) \\ & + 2\eta\xi-2\eta^2\xi^2\tanh(\eta\xi)]\Big\} \\ & + \frac{\Gamma}{2}[1-\tanh(\eta\xi)]\mathrm{sech}^2\eta\xi, \end{aligned} \tag{26}$$

where the relation of the moving coordinate system with the fixed one is

$$\begin{aligned} \overline{\theta}_\tau &= 4\eta^2+O(\mu), \\ \xi &= \theta-\overline{\theta}, \\ \Gamma &= -\frac{9}{4}\frac{H_\tau}{H}. \end{aligned} \tag{27}$$

2.2 Dispersion relation

Using an assumption that the meridional thermocline depth (Ψ) is constant, the total phase speed is

$$\begin{aligned} C_s &= (C^2 + \epsilon^{1/2}\Psi)^{1/2} \\ &\simeq C(1 + \epsilon^{1/2}\tfrac{\Psi}{2C^2} - \epsilon\tfrac{\Psi^2}{8C^4} + \ldots). \end{aligned} \tag{28}$$

In this research, however, the effect of the meridional variation of thermocline depth that causes dispersion in the Kelvin wave propagation is considered. The total phase speed becomes

$$C_s = C(1 + \epsilon^{1/2}\omega_1 + \epsilon\omega_2 + \ldots), \tag{29}$$

where ω_n are the corrections of phase speed $C(x)$. From the asymptotic solutions of orders $O(\epsilon^{1/2})$ and $O(\epsilon)$, it can be shown that :

$$\omega_1 = \frac{1}{2\sqrt{2\pi}C^2}\int_{-\infty}^{\infty} e^{-\frac{1}{2}Y^2}\Phi(Y)\,dY, \quad \text{and} \tag{30}$$

$$\omega_2 = -{\omega_1}^2 + \frac{1}{8C^4}\sum_{n=0}^{\infty} n![(n+1)\varphi_{n+2} + \varphi_n]^2, \quad \text{with} \tag{31}$$

$$\varphi_n = \frac{1}{n!\sqrt{2\pi}}\int_{-\infty}^{\infty} D_n(Y)\Phi(Y)D_o(Y)\,dY, \tag{32}$$

where $\Phi(Y) = \Psi(y)$ is the meridional variation of thermocline depth.

If the meridional thermocline depth is constant, Eqs. (29) through (32) reduce to Eq. (28). One can see that the meridional variation of thermocline depth plays an important role in the dispersion of equatorial Kelvin waves. As discussed later, a function symmetrical to the equator will constitute a favorable condition for forcing the Kelvin wave to be dispersive.

2.3 Modified Green's Law

As in the case of shallow water waves impinging on a shoaling beach, the wave amplitude increases as the depth becomes shallower. The relation between amplitude and depth has been known for more than 150 years as *Green's Law.*

Following the same procedure as in the case of a shoaling beach, from Eq. (20) yields a relation (Susanto, 1998)

$$q_\tau = -\frac{19}{8}\frac{H_\tau}{H}q, \tag{33}$$

or

$$H^{19/8}(\chi)q = I(\zeta), \tag{34}$$

which is a function of ζ only. Applying a relation of sea level deviation as $h = H^2 q$, Green's Law for an equatorial Kelvin wave in a slowly varying thermocline is

$$hH^{3/8}(\chi) = I(\zeta). \tag{35}$$

This result is the same as a modified Green's Law predicted by Long and Chang (1990), for linear and nondispersive equatorial waves.

2.4 Energy Conservation Law

Long and Chang (1990) concluded that, based on the full energy equation and the direct integration of the PKdV equation, Eq. (14), in a reduced gravity ocean, the net energy at any given x is conserved. Hence, the energy conservation law at any given x is in the following form:

$$\frac{\partial}{\partial x}E_{tot} = 0, \tag{36}$$

with

$$E_{tot} = \int_0^\infty\int_{-\infty}^{\infty}(uhH)\,dtdy, \tag{37}$$

where E_{tot} is the net energy transport at fixed x. Substituting the linear equatorial Kelvin wave solution in Eqs. (13) into Eq. (37) yields

$$\begin{aligned} E_{Kelvin} &= \frac{\partial}{\partial x}\int_0^\infty\int_{-\infty}^{\infty}(u_o h_o H)\,dtdy, \\ &= \sqrt{\pi}\frac{\partial}{\partial x}\int_{-\infty}^{\infty} H^{7/4}A^2(\zeta,\chi)\,d\zeta. \end{aligned} \tag{38}$$

This result is the same as that of multiplying Eq. (14) by A and then integrating with respect to ζ from $-\infty$ to ∞,

$$\frac{\partial}{\partial\chi}\int_{-\infty}^{\infty} H^{7/4}A^2(\zeta,\chi)\,d\zeta = 0. \tag{39}$$

Therefore, energy carried by a Kelvin wave is indeed conserved to the lowest order.

2.5 Mass Conservation Law

Unlike a periodic wave, a nonlinear equatorial wave not only transports energy, but also transports the water mass. Following a similar procedure to the conservation of energy given above, and using the linear equatorial Kelvin wave solution in Eqs. (13), the mass transport equation becomes (Long and Chang, 1990),

$$\begin{aligned} \frac{\partial}{\partial x}M_{Kelvin} &= \frac{\partial}{\partial x}\int_0^\infty\int_{-\infty}^{\infty}(u_o h_o)\,dtdy, \\ &= \sqrt{2\pi}\frac{\partial}{\partial x}\int_{-\infty}^{\infty} H^{5/4}A(\zeta,\chi)\,d\zeta. \end{aligned} \tag{40}$$

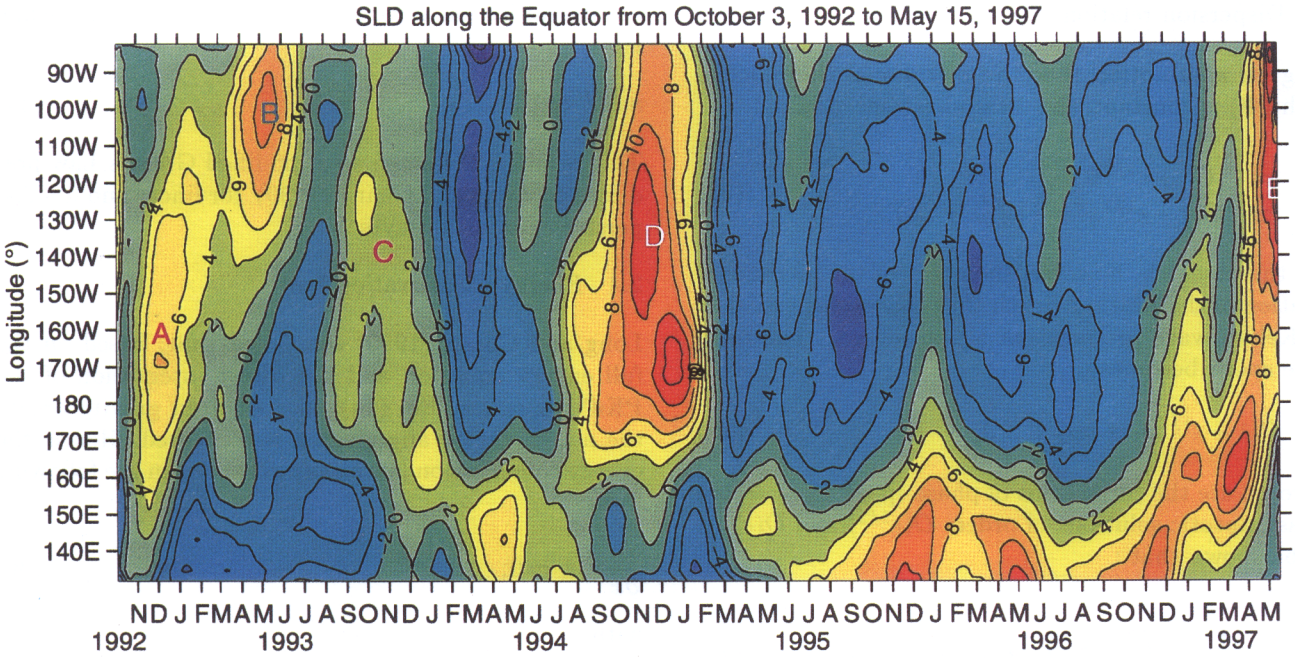

Fig. 1. Longitude-time contour plot of low-pass-filtered TOPEX/POSEIDON sea level deviation (SLD). The interval between two adjacent contours is 1 cm. The major positive peaks are coded by capital letters.

A straightforward integration of the PKdV equation, Eq. (14), with respect to ζ from $-\infty$ to ∞, however, gives

$$\frac{\partial}{\partial \chi} \int_{-\infty}^{\infty} H^{7/8} A(\zeta, \chi)\, d\zeta = 0. \tag{41}$$

One can see that there is a different power of H in Eqs. (40) and (41), implying that Eq. (40) will not be zero. This means that an equatorial Kelvin wave propagating in a slowly varying thermocline depth does not conserve its total mass at the lowest order (Long and Chang, 1990); part of the mass is reflected.

3 Comparisons of T/P Observations with Soliton Solutions of the PKdV Equation

Theories given in Section 2 will be used for comparing with T/P sea level variability signals during the period from March to June 1993 shown in Fig. 1.

From Eqs. (13) to (17), a complete expression of the upper layer thickness variability has been obtained,

$$h(\chi, Y; \theta, \tau) = \left(\frac{2}{3}\right)^{1/2} H^2(\chi) q(\theta, \tau) e^{-\frac{1}{4}Y^2}. \tag{42}$$

Previous investigators (for example Rebert et al., 1985; Zheng et al., 1995) indicate that in the equatorial oceans, the upper layer thickness variability or changes in the upper layer depth of thermocline h have a direct correlation with the sea level variability or the SLD $\tilde{h}$:

$$\tilde{h} = h \frac{\Delta \rho}{\rho}, \tag{43}$$

where $\Delta\rho/\rho$ is the relative density difference between the two layers above and below the thermocline.

The sea level variability can be determined by T/P satellite altimeters up to an accuracy of 2–3 cm. This accuracy allows the use of T/P SLD data in comparisons with theoretical predictions.

3.1 Zonal Structure

The zonal structure of SLD time series for peak B (Fig. 1) along the equator from March 1 to June 8, 1993 are shown in Fig. 2. In order to compare with the theoretical predictions in Eq. (42) and Eqs. (25) through (27), it is necessary to transform these curves plotted using the data observed in the geographic coordinate system into the new dynamical coordinate system using transformation relations Eqs. (8), (18), and (19), and $\chi = \epsilon x$. To perform this transformation, the thermocline depth $H(\chi)$ must first be determined. The monthly zonal and meridional thermocline depth data from November 1992 to June 1993 are shown in Figs. 3a and 3b, respectively. These data are obtained from The Bureau of Meteorology Research Center (BMRC) Australia which originally derived from XBT and TOGA-TAO data.

The normalized zonal thermocline depth data in March, April and May 1993 shown in Fig. 3a can be approximated by an hyperbolic tangent function (Susanto, 1998),

$$H(\chi) = h_o \left\{ 1 - \delta \tanh \left[\frac{(\chi - \chi_c)}{L} \right] \right\}. \tag{44}$$

The value of h_o depends on the choice of thermocline depth scale, H_o. For convenience in calculation, $h_o =$

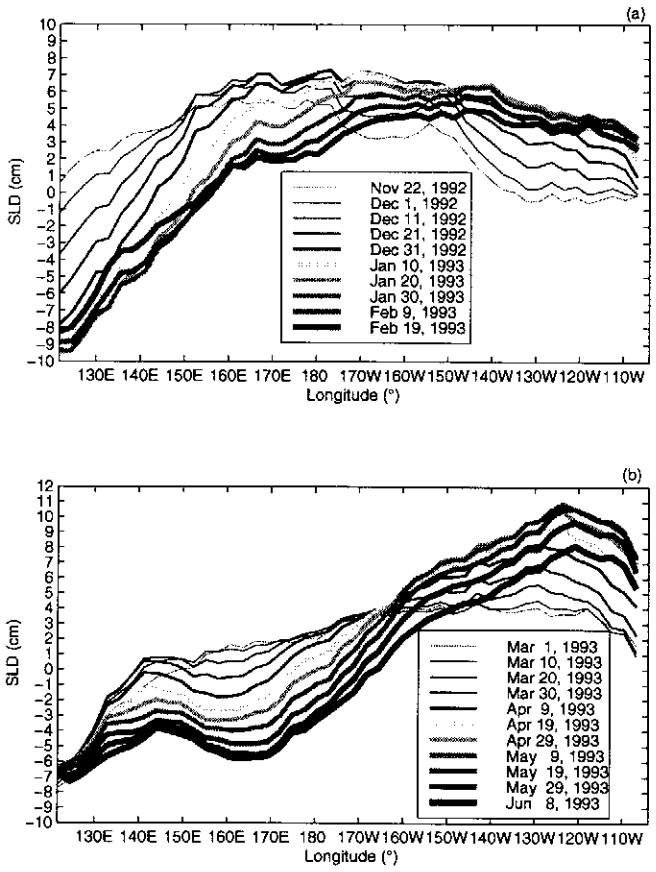

Fig. 2. The evolution of zonal SLD structure of peak B in Fig. 1 from March 1, 1993 to June 8, 1993.

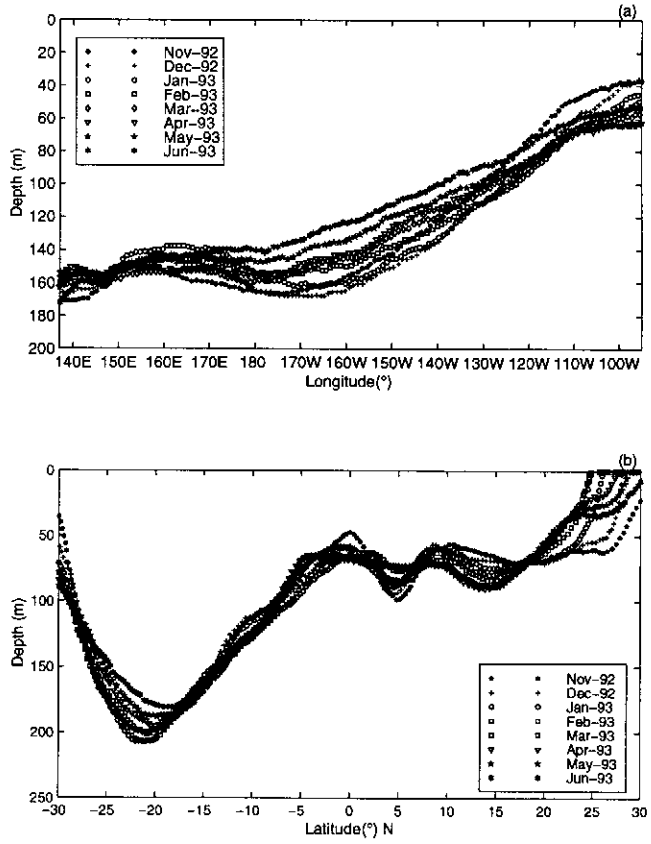

Fig. 3. Monthly mean (a) zonal and (b) meridional thermocline structures along 110° W in the equatorial Pacific from November 1992 to June 1993 obtained from BMRC-Australia. The original data derived from XBT's and TOGA-TAO data.

1. Using a curve-fitted method, the best-fitted line is achieved for the values of $\delta = 0.484$, $\chi_c = 0$ at 134° W, the zonal length scale $L = 30°$, and depth scale $H_o = 103$ m. The results are shown in Fig. 4. In this research, this hyperbolic tangent function is used in the transformation in comparing the zonal and temporal structures of solitons between the analytical solution and observation.

Comparisons of zonal T/P SLD along the equatorial Pacific of three curves in April and May 1993, with a solitary wave solution Eq. (42) and Eqs. (25) through (27) are shown in Fig. 5 and 6, respectively. The plotted symbols are derived from the T/P SLD data, while the solid lines are the theoretical results. One can see an excellent agreement between the two. Not only the major solitons fit each other, but also a tail as predicted by the 1-order solution, is seen to occur on their lee sides.

3.2 Meridional Structure

Equation (42) indicates that, like the linear equatorial Kelvin mode, the solitary Kelvin wave also has a Gaussian meridional structure. In the real ocean, however, the equatorial Kelvin wave coexists with the Rossby waves, rather than being the sole component. In order to determine the wave components in the sea level ob-

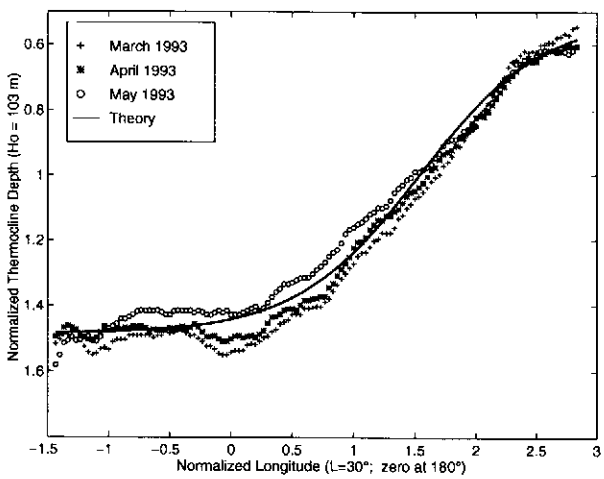

Fig. 4. Hyperbolic tangent fitting of the zonal thermoclines (normalized by 103 m) in April and May 1993. The zero reference is chosen at 180° where the thermocline begins shoaling.

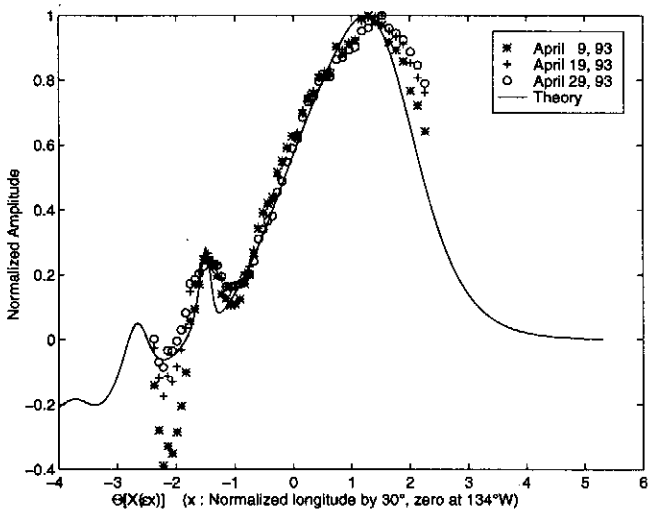

Fig. 5. Comparisons of normalized zonal SLD structure of peak B shown in Fig. 1 (data points) with the solitary solution of the PKdV equation (curve), for three cycle repeated observations in April 1993.

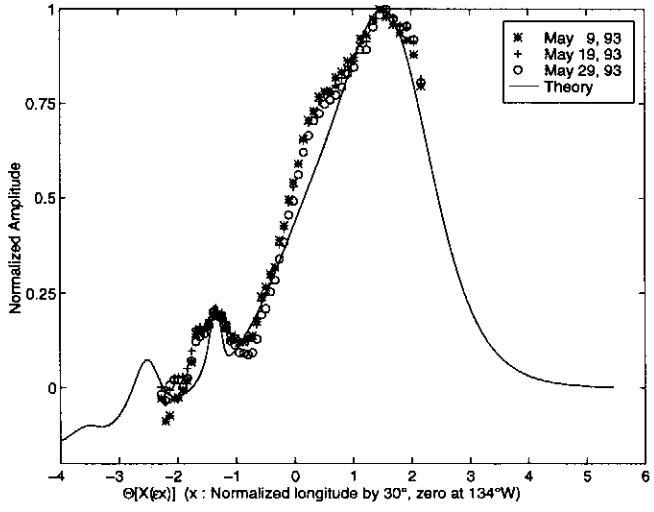

Fig. 6. Comparisons of normalized zonal SLD structure of peak B shown in Fig. 1 (data points) with the solitary solution of the PKdV equation (curve), for three cycle repeated observations in May 1993.

servations, a theoretical Kelvin-Rossby wave mode decomposition is used to expand the meridional sea level structure into parabolic cylinder functions. For SLD peak B shown in Fig. 1, the wave components in March, April, and May 1993 are computed. The parabolic cylinder functions, up to the $7th$-order, are used to fit the meridional structure of the SLD. The results are given in Fig. 7.

The amplitudes of the wave modes and phase speeds of the Kelvin mode obtained are listed in Table 1. One can see that the equatorial Kelvin mode is the primary component, and high order Rossby modes (for $n > 3$) are negligible, implying that the Kelvin wave is a dominant feature of peak B. In this table, the sea level for May 29 and June 8 are included in order to show that the amplitude of the Kelvin wave varies as it propagates eastward. The amplitude peaks at 103° W on May 9, 1993 and then it decays, at the same time the amplitude of Rossby mode 2 increases. This is probably due to the Kelvin wave transformation into westward propagating Rossby waves (Susanto et al., 1998).

Table 1. Kelvin-Rossby mode decomposition of meridional structure of sea level at locations of the peak of the solitons. K denotes the Kelvin mode and R the Rossby modes.

Date 1993	Long. (° W)	Speed ($m\,s^{-1}$)	Amplitude (cm)			
			K	R-1	R-2	R-3
March 1	122	3.1	3.26	−1.22	0.72	−1.01
March 10	120	3.2	3.69	−1.52	−0.12	−0.97
March 20	115	3.2	5.85	−1.56	−1.22	−0.84
March 30	110	3.3	9.32	−2.00	−2.46	−0.47
April 9	108	3.2	9.89	−1.40	−1.84	−0.50
April 19	106	3.2	9.58	0.00	−0.86	−0.65
April 29	104	3.3	10.19	1.54	−0.57	−0.93
May 9	103	3.3	10.44	2.11	0.11	−0.80
May 19	102	3.3	9.16	2.16	1.04	−0.67
May 29	100	3.2	7.72	1.24	2.03	−0.24
June 8	100	3.1	5.85	1.64	2.52	−0.24

3.3 Time Domain Structure

Solitary wave solutions in Eq. (42) and Eqs. (25) through (27) can also be used for comparing with sea level time series observations at a given location. In this case, the given longitude is chosen as an origin of the spatial coordinate system to simplify computing and plotting processes. Comparisons are made between sea level time series measured at three locations, 107.6° W, 104.8° W, and 102.0° W longitude and the theoretical solution at the equator, which is determined with the same parameters as used for zonal structure solution, as shown in Fig. 8. Noting that, in contrast to zonal structure, the tail of the soliton in the time domain is on the right side of the major soliton. One can see again that the observations and the theoretical solution agree very well.

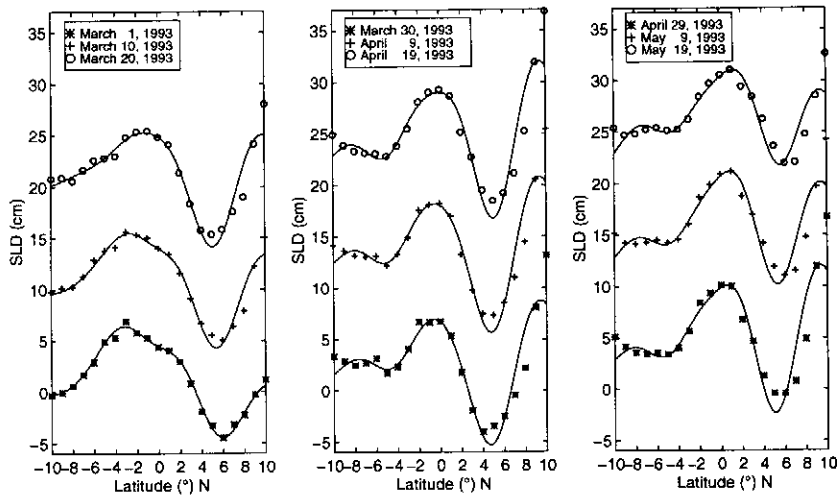

Fig. 7. The Kelvin-Rossby mode analysis for the meridional SLD structure of peak B shown in Fig. 1 from March 1, 1993 to May 19, 1993. The data points are TOPEX/POSEIDON observations, and the curves are a superposition of the Kelvin and the first six Rossby modes.

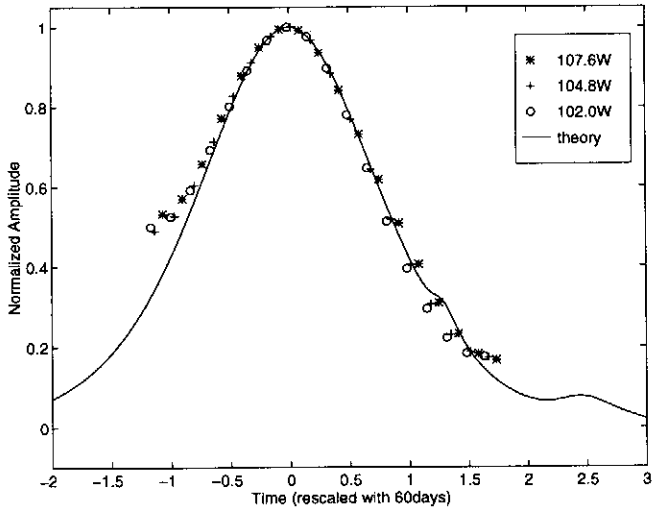

Fig. 8. Comparison of normalized SLD time series of peak B shown in Fig. 1 measured at crossings of three longitudes with the equator (data points) with the time domain solitary solution of the PKdV equation (curve).

3.4 Dispersion Relations

The meridional structure of the thermocline depth shown in Fig. 3b causes a dispersive effect in the propagation of equatorial Kelvin waves. In order to compare the dispersion relations in Eqs. (29) through (32) with sea level observations, the functional form of the meridional variation of thermocline depth $\Phi(Y)$ must first be determined. This can also be obtained by fitting the measurements. In this research, the variability of meridional thermocline depth is expressed in the form of an expansion of the parabolic cylinder functions $D_n(Y)$.

$$\Phi(Y)e^{-\frac{1}{4}Y^2} = \sum_{n=0}^{\infty} \varphi_n D_n(Y). \tag{45}$$

Using the orthogonality of parabolic cylinder functions,

$$\int_{-\infty}^{\infty} D_m(Y)D_n(Y)\,dY = \begin{cases} n!\sqrt{2\pi} & \text{if } m = n. \\ 0 & \text{otherwise.} \end{cases} \tag{46}$$

Therefore,

$$\begin{aligned} \int_{-\infty}^{\infty} D_n \Phi(Y) e^{-\frac{1}{4}Y^2}\,dY &= \int_{-\infty}^{\infty} D_n \sum_{m=0}^{\infty} \varphi_m D_m(Y)\,dY \\ &= n!\sqrt{2\pi}\varphi_n, \end{aligned} \tag{47}$$

and hence,

$$\varphi_n = \frac{1}{n!\sqrt{2\pi}} \int_{-\infty}^{\infty} D_n(Y)\Phi(Y)D_o(Y)\,dY. \tag{48}$$

Using Eq. (48), φ_n can be determined. Based on the maximum peak B, which is at 110° W (Fig. 1), the variation of the meridional thermocline depth at this longitude for March, April, and May 1993, are expanded into parabolic cylinder functions up to the $7th$-order to approximate the definite integral in Eq. (48). The results are shown in Fig. 9. The meridional variation of thermocline depth is multiplied by a filter function $D_o = e^{-Y^2/4}$ as in Eq. (45) prior the parabolic cylinder function decomposition. The values of φ_0 to φ_3 for March, April, and May 1993 are listed in Table 2.

Table 2. Decomposition of meridional thermocline depth into parabolic cylinder functions (D_n) with a filter function $D_o = \exp(-\frac{1}{4}Y^2)$.

Month 1993	Amplitude				M
	φ_o	φ_1	φ_2	φ_3	
March	0.7539	−0.127	0.094	−0.016	0.021
April	0.7540	−0.105	0.102	−0.019	0.018
May	0.7655	−0.100	0.094	−0.020	0.016

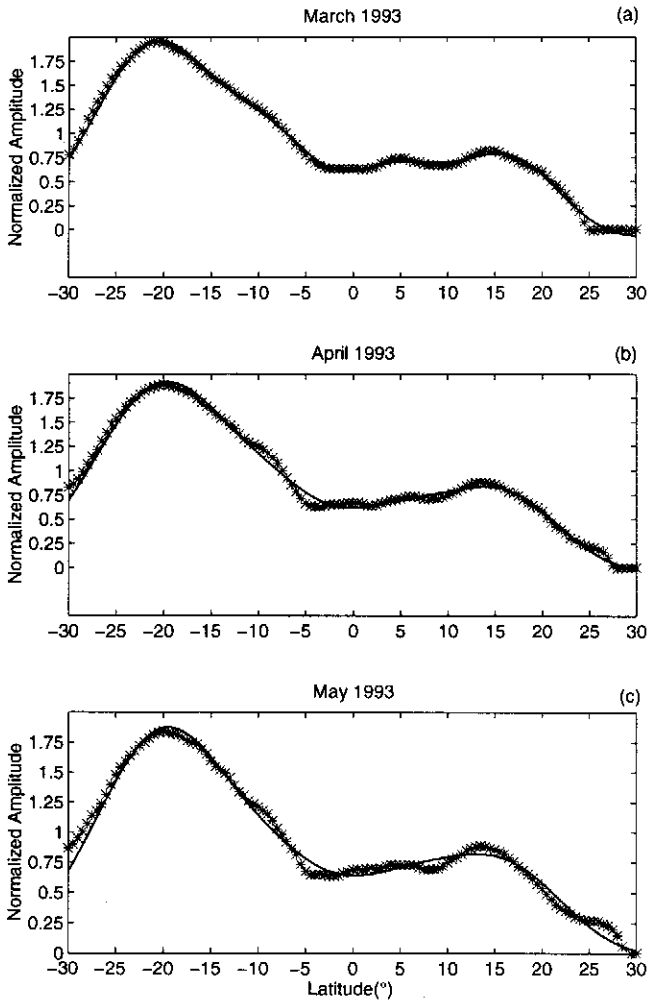

Fig. 9. Parameterization of the meridional structure of the thermocline along 110° W. (a) For the thermocline depth in March 1993, (b) April 1993, and (c) May 1993. The curves are a superposition of the first four parabolic cylinder functions.

From Table 2, one can see that φ_o is most dominant, while φ_n, for $n > 3$, are negligible. The averaged values of φ_o to φ_3 are 0.76, −0.11, 0.10, −0.02, respectively. M measures the dispersion strength, which is calculated using Eqs. (15) and (16) or Eq. (48) and its average value is 0.018.

Applying the relation in Eq. (47) to Eq. (30) yields,

$$\omega_1 = \frac{\varphi_o}{2H}, \tag{49}$$

hence, the dispersion relations in Eqs. (29) through (32) can be expressed as (Susanto, 1998)

$$\begin{aligned} C_s &= \sqrt{H(\chi)}\left[1 + \frac{\alpha}{H(\chi)} + \frac{\alpha^2}{2H^2(\chi)}\left(\frac{\gamma}{{\varphi_o}^2} - 2\right)\right] \\ &= \sqrt{H(\chi)}\left[1 + \frac{\alpha}{H(\chi)} + \frac{\Delta}{2}\frac{\alpha^2}{H^2(\chi)}\right], \end{aligned} \tag{50}$$

where

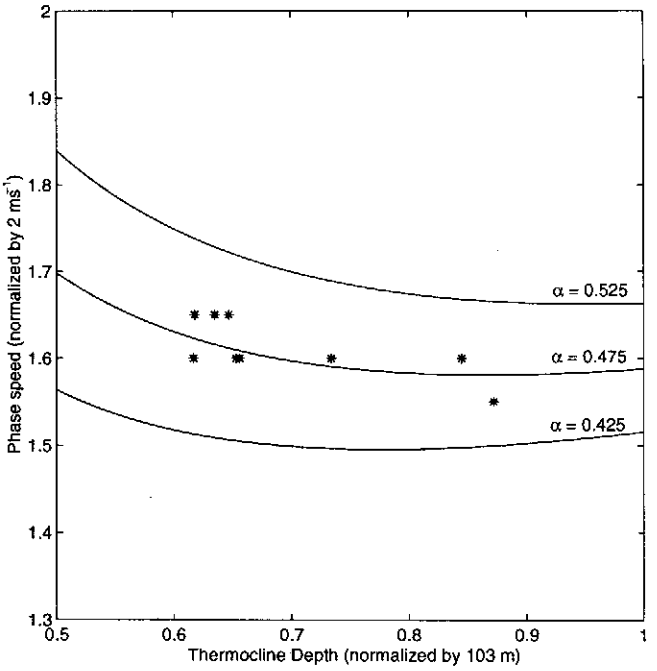

Fig. 10. Dispersion relation of the equatorial Kelvin solitary waves. Curves represent the theoretical results with parameter α as 0.525, 0.475, and 0.425, respectively. The data points represent normalized phase speeds derived from the meridional SLD structure of peak B shown in Fig. 1 from March 1, 1993 to May 19, 1993.

$$\begin{aligned} \alpha &= \frac{\epsilon^{1/2}\varphi_o}{2}, \\ \Delta &= \left(\frac{\gamma}{{\varphi_o}^2} - 2\right), \\ \gamma &= \sum_{n=0}^{\infty} n![(n+1)\varphi_{n+2} + \varphi_n]^2. \end{aligned} \tag{51}$$

Equation (50) represents a family of curves with α as a parameter as shown in Fig. 10. Based on the values of φ_o through φ_3, $\gamma = 0.7850, 0.7961, 0.7999$ and $\Delta = -0.6190, -0.5996, -0.6351$ for March, April, and May 1993, respectively. The data points represent normalized phase speeds determined with meridional variations of the sea level shown in Fig. 7. Normalized thermocline depth is calculated with measurements shown in Fig. 3 in March, April, and May 1993, and at the locations where the peaks of solitons are located. One can see that the data points determined with measurements are close to those on the theoretical curve with $\alpha = 0.475$, implying the solitary nature of studied equatorial Kelvin waves. From the values of α and φ_o, we have $\epsilon = 0.0326$, which indeed satisfies $\epsilon \ll 1$. Hence, the assumption of the perturbation expansion holds.

3.5 Modified Green's Law

Equation (35) indicates that, for a given initial condition $I(\zeta)$, the amplitude of a soliton should be inverse

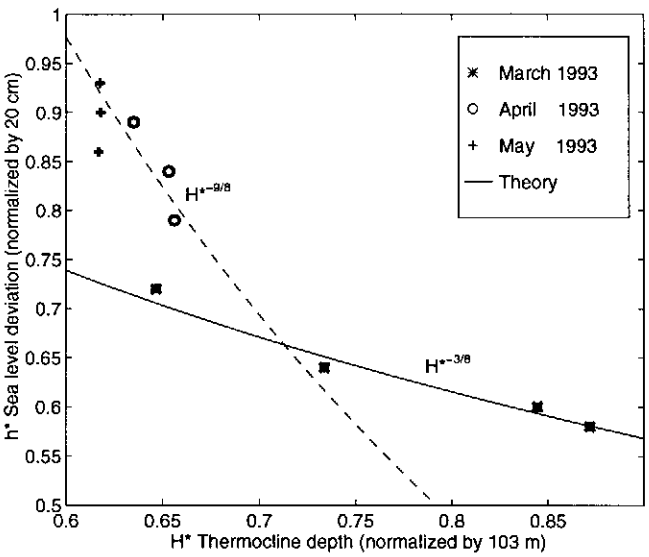

Fig. 11. Dependence of the amplitude of Kelvin soliton on thermocline depth. The data points are determined by observations: SLD amplitudes of Kelvin solitons and thermocline depths at the locations of the peaks of solitons. The solid line is Green's Law. The dashed line is the curve-fit for April and May 1993.

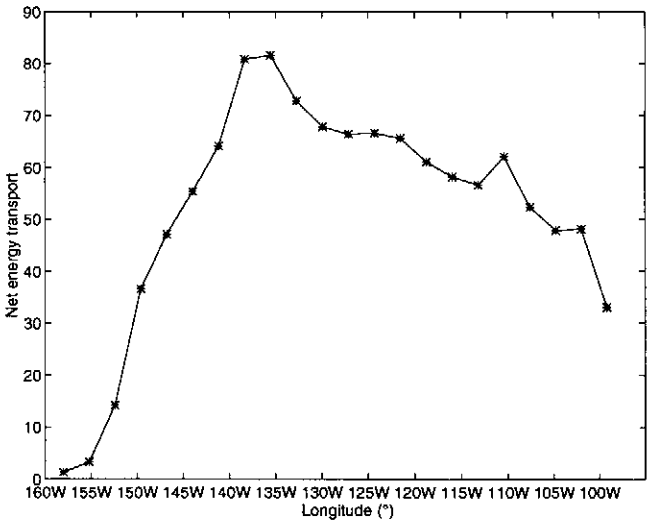

Fig. 12. Energy Variability. In the early development of an equatorial solitary Kelvin wave, the net energy transport increases, then starting from 140° W the energy gradually decays.

proportionality to $H^{3/8}$. This inverse proportionality relation can be shown as curves in the Fig. 11. $I(\zeta)$ is chosen as 0.472 for fitting the data of March 1993. The measured data, the amplitudes of solitons from Fig. 2, and the thermocline depths from Fig. 3a, are shown in Fig. 11 as different symbols. One can see that the data of March 1993 agree very well with the theoretical curve.

It seems that, for the early development of a solitary wave, an inverse proportionality relationship between sea level and thermocline depth $H^{3/8}$ holds. However, for further development, data from April and May 1993 do not follow the same trend. As expected, the shallower the thermocline depth, the higher SLD and the higher the nonlinearity effect. Green's Law of $hH^{3/8}$ constant is obtained based on the linear approximation of the nonlinear equation of PKdV, Eq. (20). Therefore, this relation works well in the early development of a solitary equatorial wave or at a location where the thermocline starts to change. For the shallower region, the power of H should increase. Based on the curve-fitted data, the relation should be $H^{9/8}$ and $I(\zeta) = 0.8$, which is shown as the dashed line in Fig. 11. In the case of gravity waves approaching a beach with a slowly changing water depth, this phenomenon has been predicted by many investigators (for example, Shuto, 1974; Miles, 1977, 1979), where the relation of the normalized wave amplitude and depth, ηH^1 is constant.

3.6 Energy Conservation Law

Equations (38) and (39) indicate that the net energy transport carried by the equatorial Kelvin wave at any given x is constant. As mentioned earlier, the T/P SLD data during the period of March to June 1993 shown in Fig. 1 will be used to compare with the theory. Therefore, the time integration limit from $-\infty$ to ∞ in Eqs. (38) and (39) are approximated by a summation of nine data points from March 1 to May 19, 1993. In order to investigate the energy conservation, first the meridional structure of SLD during this time period is decomposed into Kelvin-Rossby wave modes and then the Kelvin mode amplitude and its normalized phase speed are obtained. This decomposition is carried out for each longitude from 158° W to 99.2° W with an increment of 2.8° longitude. Hence, we have Kelvin wave component h_{oi} and its normalized phase speed c_{oi}, where $i = 1, \ldots, 9$ for each given longitude. The next step is calculate the normalized thermocline depth for March, April, and May 1993 at each longitude given above. Since only a monthly thermocline depth is available, we have to assume that there is no thermocline depth change within a month. Then $\sum_i^{N=9}(h_{oi}/{c_{oi}}^2){H_i}^{7/4}$ is calculated. The results are shown in Fig. 12. One can see that at westside of 140° W a Kelvin wave starts to be generated, hence, the energy increases. However, from 140° W to the east the net energy transport of the Kelvin wave is not constant, implying that its energy is not conserved. This result indicates that the net energy transport carried by the Kelvin wave gradually decays as it propagates eastward. This does not agree with that predicted by Long and Chang (1990). The energy loss is may due to the energy transfer between vertical modes as predicted by Gill and King (1985).

3.7 Mass Conservation Law.

As in the energy conservation law, the mass transport is calculated based on Eqs. (40) and (41). The results are shown in Fig. 13. One can see that in the early

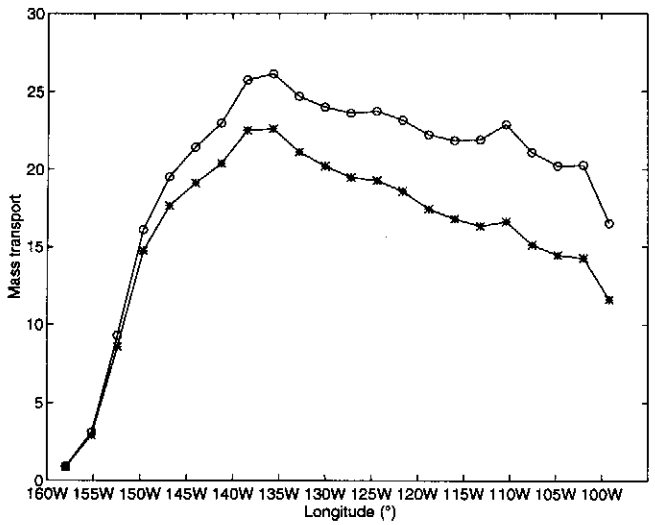

Fig. 13. Mass Variability. Based on the mass conservation law (open-circle curve) and based on the PKdV equation (asterisks curve).

development of a Kelvin wave, the mass transport increases and both equations give the same results. Then, as the the thermocline depth becomes shallower, the difference between those equations becomes larger indicating that the reflected water mass increases. Hence, these results agree well with that predicted by Long and Chang (1990).

4 Disscussions and Conclusions

TOPEX/POSEIDON altimeter sea level deviation time series data and thermocline depth data derived from XBT and TOGA-TAO measurements are used to investigate the behaviors of equatorial Kelvin solitary wave along an eastward shoaling thermocline in the equatorial Pacific during the 1992-1993 El Niño. Our results show is that under a varying thermocline, the equatorial Kelvin solitary waves, which were theoretically predicted by Boyd (1984) and Greatbatch (1985), indeed exist in the real ocean.

The hyperbolic tangent function is used to approximate the zonal shoaling thermocline along the equator. Following Long and Chang (1990), a $1\frac{1}{2}$-layer reduced-gravity ocean model with no mean background current is used for simulating the equatorial Pacific. Applying multiple scale and perturbation expansion analyses, the solutions using an asymptotic expansion up to second order are obtained. The behaviors of the waves observed as they propagate along the eastward shoaling thermocline depth can be approximately described with the solutions of the PKdV equation and the modified Green's Law. They are characterized by the following points: (1) The meridional sea level structure can be described by the Gaussian function, the same as that of linear Kelvin waves; (2) The zonal sea level structure consists of a single major soliton, which can be described by a hyperbolic secant function, and a tail in the lee side of the major soliton; (3) The structure in the time domain is the same as the zonal structure; (4) The phase speed depends on the local thermocline depth and its meridional variation; (5) In the early stages, the amplitude increases as the thermocline depth decreases to the power $-3/8$. Our observations show that the relation between the amplitude of solitary Kelvin wave and the thermocline depth does follow Green's Law, only before the wave approaches a very shallow thermocline. In that case, the power of H determined by curve fitting is $-9/8$, which is much higher than $-3/8$ given by Green's Law. This phenomenon may be explained by the increase of nonlinear effects with thermocline's shoaling. Neither mass nor energy are conserved; part of the water mass is reflected. The energy likely transfers from lower mode to higher modes as predicted numerically by Gill and King (1985).

The T/P SLD observations shown in Fig. 2 also suggest that the eastern boundary of the ocean basin may have an influence on the evolution of equatorial Kelvin waves. Examining the figure and Table 1, one can see that the amplitude of the soliton gradually decreased after May 9, 1993. This phenomenon indicates that the wave began decaying. A parallel study shows the reason for this decay is the transfer of energy and mass to the Rossby waves due to the reflectance of the wave at the eastern boundary (Susanto et al., 1998).

Acknowledgements. The work is supported by NASA's TOPEX/POSEIDON Altimeter Research Program (Application for Studies of Ocean Dynamics) through a subcontract with Dr. Chang-Kou Tai at the NOAA Geoscience Laboratory and NASA Scatterometer (NSCAT) and NASA Earth Observing System (EOS) Interdisciplinary Science Investigations program. The author would like to thank Robert Cheney, NOAA Geoscience Laboratory for providing the T/P data. We would like to thank anonymous reviewers for their fruitful comments, James Kirby for his helpful discussions and Simon Shaw for preparing the paper.

References

Boyd, J. P., Equatorial solitary waves, part 1: Rossby solitons, *J. Phys. Oceanogr., 10*, 1699–1717, 1980.

Boyd, J. P., Equatorial solitary waves, part 2: Envelope solitons, *J. Phys. Oceanogr., 13*, 428–449, 1983.

Boyd, J. P., Equatorial solitary waves, part 4: Kelvin solitons in a shear flow, *Dyn. Atmos. Oceans, 8*, 173–184, 1984.

Boyd, J. P., Nonlinear equatorial waves, in *Nonlinear Topics in Ocean Physics*, edited by A. R. Osborne and L. Bergamosco, pp. 51–97, 1990.

Busalacchi, A. J. and Cane, M. A., The effect of varying stratification on low-frequency equatorial motions, *J. Phys. Oceanogr., 18*, 801–812, 1988.

Cushman-Roisin, B., *Introduction to geophysical fluid dynamics*, Prentice Hall, New Jersey, 1994.

Eriksen, C. C., Blumenthal, M. B., Hayes, S. P., and Ripa, P., Wind-generated equatorial Kelvin waves observed across the Pacific ocean, *J. Phys. Oceanogr., 13*, 1622–1640, 1983.

Gill, A. E., *Atmosphere ocean dynamics*, pp. 429–491, Academic Press, 1982.

Gill, A. E. and King, B. A., The effect of a shoaling thermocline on equatorially-trapped Kelvin waves. *dynamical climatology*, Tech. Note: DCTN 27, Meteorological Office, Berkshire, UK., 1985.

Glazman, R. E., Frabrikant, A., and Greysukh, A. M., Nonlinear features of equatorial baroclinic Rossby waves detected in Topex altimeter observations, *Nonlin. Proc. Geophys.*, *3*, 115–126, 1996.

Greatbatch, R. J., Kelvin wave fronts, Rossby solitary waves and the nonlinear spin-up of the equatorial oceans, *J. Geophys. Res.*, *90*, 9097–9107, 1985.

Hughes, R. L., The influence of thermocline slope on equatorial thermocline displacement, *Dyn. Atmos. Oceans*, *5*, 147–157, 1981.

Kindle, J. C., On the generation of Rossby solitons during El Niño, in *Hydrodynamics of the Equatorial Oceans*, edited by J. C. Nihoul, pp. 353–368, Elsevier Oceanogr. Ser, Elsevier, New York, 1983.

Knox, R. A. and Halpern, D., Long range wave propagation of transport variation in Pacific ocean equatorial currents, *J. Mar. Res.*, *40*, 329–339, 1982.

Long, B. and Chang, P., Propagation of an equatorial Kelvin waves in a varying thermocline, *J. Phys. Oceanogr.*, *20*, 1826–1841, 1990.

Lukas, R., Hayes, S. P., and Wyrtki, K., Equatorial sea level response during the 1982–1983 El Niño, *J. Geophys. Res.*, *89*, 10,425–10,430, 1984.

Marshall, H. G. and Boyd, J. P., Solitons in a continuously stratified equatorial ocean, *J. Phys. Oceanogr.*, *17*, 1016–1031, 1987.

Maxworthy, T., Experiments on solitary internal Kelvin waves, *J. Fluid Mech.*, *129*, 365–383, 1983.

Melville, W. K., Renouard, D. P., and Zhang, X., On the generation of nonlinear internal Kelvin waves in a rotating channel, *J. Geophys. Res.*, *95*, 18,247–18,254, 1990.

Miles, J. W., Note on a solitary wave in a slowly varying channel, *J. Fluid Mech.*, *80*, 149–152, 1977.

Miles, J. W., On the Korteweg-de Vries equation for a gradually varying channel, *J. Fluid Mech.*, *91*, 181–190, 1979.

Moore, D. W. and Philander, S. G. H., Modeling of the tropical oceanic circulation, *The Sea*, *6*, 319–361, 1977.

Newell, A. C., *Soliton in mathematics and physics*, Society for Industrial and Applied Mathematics, Philadelphia, 1985.

Pedlosky, J., *Geophysical fluid dynamics*, Springer-Verlag, New York, 2nd edn., 1987.

Philander, S. G., *El Niño, La Niña, and Southern Oscillation*, Academic Press, San Diego, 1990.

Rebert, J. P., Donguy, J. P., Eldin, G., and Wyrtki, K., Relation between sea level, thermocline depth, heat content, and dynamics height in the tropical Pacific ocean, *J. Geophys. Res.*, *90*, 11,719–11,725, 1985.

Renouard, D. P., D'Hieres, G. C., and Zhang, X., An experimental study of strongly nonlinear waves in a rotating system, *J. Fluid Mech.*, *177*, 381–394, 1987.

Ripa, P. and Hayes, S. P., Evidence for equatorial trapped waves at the Galapagos islands, *J. Geophys. Res.*, *86*, 6509–6516, 1981.

Shen, S. S., *A course on nonlinear waves*, Kluwer Academic Pub., Boston, 1993.

Shuto, N., Nonlinear long waves in a channel of variable section, *Coastal Engineering in Japan*, *17*, 1–12, 1974.

Susanto, R. D., *Observation and dynamical analysis of equatorial waves in the Pacific Ocean*, Ph.D. thesis, Univ. of Delaware, 1998.

Susanto, R. D., Zheng, Q., and Yan, X.-H., Complex singular value decomposition analysis of equatorial waves observed by TOPEX/POSEIDON altimeter, *J. Atmos. Ocean. Technol.*, *15*, 764–774, 1998.

Zheng, Q., Yan, X.-H., Ho, C.-R., and Tai, C.-K., Observation of equatorial trapped waves in the Pacific using geosat altimeter data, *Deep-Sea Res.*, *42*, 797–817, 1995.